RESEARCH ARTICLE | NOVEMBER 10 2003

Electron-Impact Cross Sections and Energy Deposition in Molecular Hydrogen

W. T. Miles; R. Thompson; A. E. S. Green

J. Appl. Phys. 43, 678–686 (1972)
https://doi.org/10.1063/1.1661176

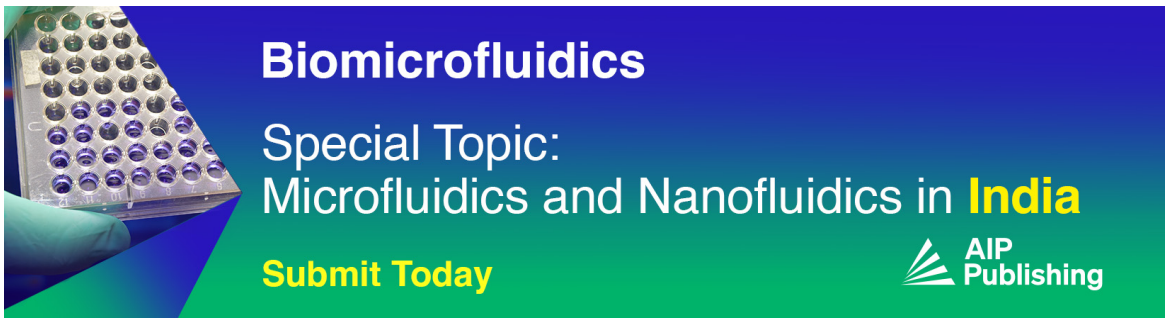

particle; the probability for this per τ seconds is $\sim\gamma(c/n)^{k^2}$, where γ is the number of possible locations of the disk and $\sim k^2$ sites must be simultaneously occupied by voids. Therefore, the number of jumps per sec with lateral component $2a$ is $\sim\nu\gamma(c/n)^{k^2}$, and we have

$$D_k' = \tfrac{1}{2}\nu\gamma(c/n)^{k^2}(2a)^2 \approx D'\gamma(c/n)^{k^2-1}. \quad \text{(C5)}$$

Since c/n is small compared with unity and $\gamma \lesssim k^2$, D_k' decreases rapidly with increasing k. Using D_k' in the discussion leading to Eq. (C4) we obtain instead

$$\left(\frac{\gamma(c/n)^{k^2-1}\,\Delta z}{z}\right)^{1/2} \ll 1, \quad \text{(C6)}$$

so that for $k \sim 2$ or 3, we expect the foreign particle to behave very nearly as an ideal marker all the way to the orifice.

[1] J. M. Rausch, Ph. D. thesis (Princeton University, 1949) (unpublished).

[2] D. C. Drucker and W. Prager, Quart. Appl. Math. 10, 157 (1952).

[3] O. Richmond and G. C. Gardner, Chem. Eng. Sci. 17, 1071 (1962).

[4] A. H. Cottrell, *The Mechanical Properties of Matter* (Wiley, New York, 1964), p. 317.

[4a] A. W. Jenike, J. Appl. Mech. 86, 5 (1964); J. R. Johanson, J. Appl. Mech. 86, 499 (1964); G. C. Gardner, Chem. Eng. Sci. 21, 261 (1965).

[5] P. G. Shewmon, *Diffusion in Solids* (McGraw-Hill, New York, 1963), p. 123.

[6] The diameter of the tower is supposed to be several times that of the orifice. Further, Rausch's complete equations (Ref. 1, p. 54) contain additional factors which turn out to be insignificant in the present case.

[7] Harold Cramér, *Mathematical Methods of Statistics* (Princeton U. P., Princeton, N. J., 1946), Chap. 15.

[8] The general case of biased random flights in which there are nonzero mixed second moments has been treated by Chandrasekhar (Ref. 10). His treatment needs to be corrected, however, since it shows the variance of the resultant pdf after N jumps (and hence the corresponding $2Dt$) to be N times the second moment (generally incorrect) rather than N times the variance (correct) of the pdf for an individual jump. The necessary revision of the treatment is given in Appendix A.

[9] Reference 7, p. 213.

[9(a)] If $\langle\rho^2\rangle$ is given, the D's and V cannot be independently chosen; adding Eqs. (3.3c, d), and using Eqs. (3.2c, d) as well as Eq. (3.3b), it is easily seen that $D_x+D_y+D_z = \frac{1}{2}\nu[\langle\rho^2\rangle - \langle w\rangle^2] = \frac{1}{2}\nu\langle\rho^2\rangle - (1/2\nu)V^2$.

[10] S. Chandrasekhar, Rev. Mod. Phys. 15, 15 (1945).

[11] H. S. Carslaw and J. C. Jaeger, *Conduction of Heat in Solids* (Oxford U. P., London, 1959), 2nd ed., p. 42.

[12] Reference 11, p. 267.

[13] Reference 11, p. 9.

[14] Reference 11, p. 258.

[15] A more realistic restriction might be represented by the factor $U[\theta/\theta_c]$, where θ_c is the angle of repose.

[16] F. A. Zenz and D. F. Othmer, *Fluidization of Fluid-Particle Systems* (Rheinhold, New York, 1960), Chap. 2.

[17] Reference 11, p. 460.

[18] *Bateman Manuscript Project* (McGraw-Hill, New York, 1954), Vol. 1, p. 185, No. 25, using the substitution $2\beta^{1/2}t^{1/2} = R$, $pt = \lambda^2\alpha z$.

[19] Reference 11, p. 194.

[20] Reference 11, p. 493.

[21] Reference 11, p. 267.

[22] E. T. Whittaker and G. N. Watson, *A Course of Modern Analysis* (Cambridge U. P., Cambridge, England, 1927), 4th ed., p. 253.

[23] Reference 11, p. 276.

Electron-Impact Cross Sections and Energy Deposition in Molecular Hydrogen*

W. T. Miles, R. Thompson,† and A. E. S. Green
University of Florida, Gainesville, Florida 32601
(Received 21 April 1971; in final form 6 July 1971)

Using the concept of the generalized oscillator strength in the Born-Bethe approximation together with semiphenomenological techniques previously developed, we synthesize a diverse body of experimental and theoretical data on molecular hydrogen into sets of analytical electron-impact cross sections. We include in our analysis discrete, vibrational, and dissociative excitations, together with direct and dissociative ionization. Once the important cross sections are known, it is then possible to trace the energy degradation of an incident electron upon molecular hydrogen. We give results for the electron loss function, efficiencies, and eV/ion pair together with comparison to available experimental data.

I. INTRODUCTION

Electron-impact cross sections for molecular processes have been found to play an important role in the study of atmospheric phenomena, photochemistry, plasmas, and applied atomic physics. Of particular significance to such applications are the physical processes involved in the energy deposition of these electrons, i.e., how an energetic electron incident upon a gas populates the various atomic and molecular states it can excite. In order to carry out such a program in a microscopic fashion, however, it is first necessary to have at one's disposal the relevant cross sections for the various processes of interest. We take as our starting point the Born-Bethe approximation[1] in which the concept of generalized oscillator strengths plays a central role. This approximation is then modified at low energies by phenomenological techniques[2] to take into account depar-

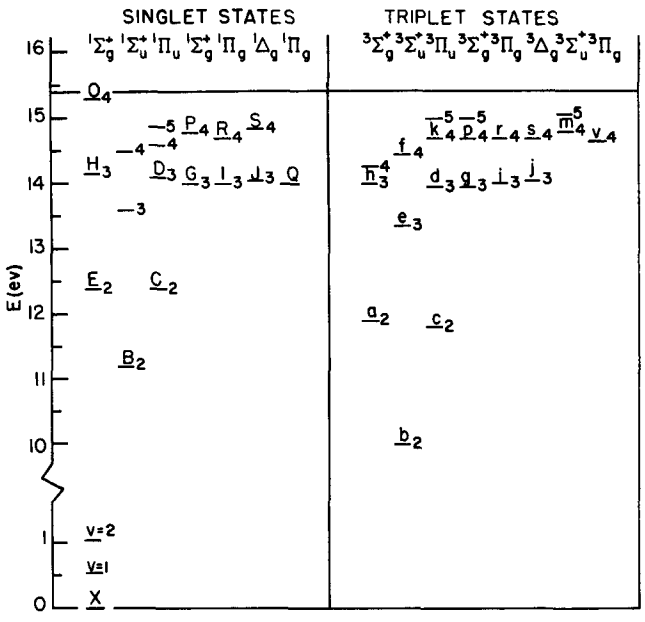

FIG. 1. Energy-level diagram for H_2. The solid line refers to the ionization threshold. $v=1$ and $v=2$ refer to the lowest vibrational states in H_2. Spectroscopic notation for the states is the same as found in Table I.

tures from the Born approximation. These are due, in part, to the effects of exchange, polarization, and distortion of the incoming and outgoing plane waves in the field of the scattering atom or molecule. Once all the important collision cross sections are assembled, the electron loss function can be determined. The ionization yield is then calculated within the framework of the continuous-slowing-down approximation[3] which allows us to trace the energy deposition of an energetic primary electron incident upon some atomic or molecular species.

In the present work we choose to study the various energy degradation processes in molecular hydrogen. Our interest in molecular hydrogen stems from the fact that as the simplest molecule it is amenable to detailed theoretical calculations and, in addition, will hopefully serve as a guide to an understanding of more complex molecules. Recent attention[4] has also been focused on the ability to achieve stimulated emissions in H_2 between 1520 and 1615 Å. Such a laser is expected to be useful for studying chemical reactions and the interaction of high-energy photons with matter. The deposition of energy in molecular hydrogen also has direct application to studies of the Jovian atmosphere in which H_2 is the predominant species.

II. DISCRETE STATES

In determining the cross sections for the various singlet states of H_2 as shown in Fig. 1, we have made use of the data of Lassettre and Jones[5] for differential cross section vs energy loss. Unfortunately, these data are not well resolved. One must, therefore, treat the bound states as continua or attempt to resolve the individual energy levels. In this work the latter is attempted.

Recent calculations[6] of electron-impact cross sections for exciting the lowest triplet states in H_2 indicate that the magnitude of the total cross section falls off rapidly with increasing n. We therefore concern ourselves with extracting the cross sections for only the low-lying singlet $B^1\Sigma_u^+$ and $C^1\Pi_u$ states from the differential cross-section data.

In order to obtain generalized oscillator strengths for these states, we have taken the shape of the experimental response function[7] to be the derivative of the Fermi function due to its analytic properties. We now say that the number of electrons per unit energy loss that one measures in an actual experiment is given by

$$\frac{dN}{dW}=\int_0^\infty L(W,W')N_{\text{true}}(W')dW' \quad , \tag{1}$$

where $L(W,W')$ is the probability of measuring an electron whose true energy loss is W' at an energy between W and $W+dW$. We normalize $L(W,W')$, i.e.,

$$\int_0^\infty L(W,W')dW'=1 \quad . \tag{2}$$

Now, since $N(W)\propto f(W)$ the oscillator strength, we can write

$$\frac{df}{dW}=\int_0^\infty L(W,W')f_{\text{true}}(W')dW' \quad . \tag{3}$$

But we also know that f_{true} is given by

$$f_{\text{true}}(W')=\sum_{B,C}\delta(W'-W_{B,C})f_{B,C}(W_{B,C})\,\text{FC}(W_{B,C}) \quad , \tag{4}$$

Hence

$$\frac{df}{dW}=\sum_{B,C}L(W,W_{B,C})f_{B,C}(W_{B,C})\,\text{FC}(W_{B,C}) \tag{5}$$

with

$$L(W,W_{B,C})=-\eta(W_{B,C})\frac{d}{dW}\left[1+\exp\left(\frac{W-W_{B,C}}{\alpha}\right)\right]^{-1} \quad , \tag{6}$$

where $\alpha=0.284$ eV corresponds to a full width at $\frac{1}{2}$ eV and

$$\eta(W_{B,C})=1+\exp[-W_{B,C}/\alpha] \quad . \tag{7}$$

Since the Franck-Condon factors are known with good accuracy,[8] df/dW is given by Lassettre and Jones[5] and $L(W,W')$ is determined, $f_{B,C}(W_{B,C})$ can be obtained by fitting to the data. We represent the oscillator strength obtained in this way by the simple analytic form[2]

$$f(\xi)=\sum_s f_s\xi^s\exp(-\alpha_s\xi) \quad . \tag{8}$$

In Eq. (8), $\xi\equiv x/x_t$ with $x=a_0^2K^2$, a_0 is the Bohr radius; K is the momentum transfer, x_t is a scaling factor given by $x_t=W/R_e$, W is the energy of a particular state, and R_e is the Rydberg energy (13.6 eV). The quantities f_s and α_s are adjustable parameters and it is found that good fits to the oscillator strengths are obtained by use of only the first term in Eq. (8). An examination of the energy level diagram for H_2 shows, however, that the $C^1\Pi_u$ and $E^1\Sigma_g^+$ states are approximately degenerate and,

TABLE I. Generalized oscillator strength parameters for singlet states.

State	W (eV)	x_t	f_0	α_0
$B^1\Sigma_u^+$	11.37	0.835	0.29	2.75
$C^1\Pi_u$	12.40	0.912	0.30	2.75
$E^1\Sigma_g^+$	12.40	0.912	0.08	2.75

hence, both contribute to the oscillator strength for the C state in our analysis. It is possible, however, to apportion the oscillator strengths for these two states by making use of Born-approximation results[9] whereby the total cross section is related to the oscillator strength via the expression[2]

$$\sigma_{\text{Born}}=\frac{q_0}{WE}\int_{\xi_{\min}}^{\xi_{\max}}\frac{f(\xi)}{\xi}\,d\xi \quad , \tag{9}$$

where $q_0=\pi a_0^2(2R_e)^2=6.514\times10^{-14}$ cm^2 eV^2 and $W(E)$ are loss (impact) energies, respectively. The final parameters for the B, C, and E oscillator strengths are given in Table I.

Once the generalized oscillator strengths are in the form of Eq. (8) it is possible to generate Born cross sections over a wide energy range through the use of Eq. (9). For low incident energies the Born approximation is no longer valid, however, and we have attempted to account for this by incorporating phenomenological distortion factors into the generalized oscillator strengths. Our method of parametrizing distortion effects and our estimates of the distortion parameters are discussed at length in Ref. 2 and will not be presented here. In Fig. 2 we show our calculated cross sections for excitation to the $B^1\Sigma_u^+$ and $C^1\Pi_u$ states. Also shown are the results of a semiclassical calculation by Prok *et al.*[9] based on the method of Gryzinski.[10] This approach includes both direct and exchange contributions to the total cross section. The agreement between our results obtained from electron-impact data and the Gryzinski estimates of Prok *et al.* for the $B^1\Sigma_u^+$ and $C^1\Pi_u$ states (note that our C state is compared with the Gryzinski estimate for the sum of the C and $E^1\Sigma_g^+$ states since in our analysis, both states are lumped together) is gratifying.

While it is not clear from the experimental data of Lassettre[5] as to whether or not there is substantial oscillator strength in the region from 12 to 15 V, it is well known that at low energies the triplet states can play an important role in the energy-loss process. This is because in the energy-deposition problem, although the energies of the primaries may be high, the resultant secondaries, tertiaries, etc. will appear in the very-low-energy region. Accordingly, it is important to take into account the triplet states, if only in some approximate fashion. In this regard we make use of some recent theoretical and experimental studies of Kuppermann and co-workers[6,11] as well as the previously mentioned[9] Gryzinski estimates for the low-lying triplet states in H_2. In order to conveniently include these triplets as well as the singlet cross sections in later energy degradation calculations, we represent them in the form

$$\sigma=\frac{q_0 A}{W^2}\left(\frac{W}{E}\right)^{\Omega}\Phi \quad , \tag{10}$$

$$\Phi=\begin{cases}1-(W/E)^{\gamma}\\ [1-(W/E)]^{\nu}\end{cases} \tag{11}$$

similar to the one used by Green and Barth.[12] Here A, Ω, γ, and ν are adjustable parameters to be fit to the data. For the singlet states $(W/E)^{\Omega}$ accurately simulates the $E^{-1}\ln E$ dependence of the Born approximation, Φ provides for the threshold behavior of the cross section, and A is a normalization constant. For the triplet states we choose the first form of Φ in Eq. (11) with $\gamma=3$ while the singlet states are best represented by the latter form with $\nu=3$. The most important cross sections in the triplet system of H_2 are the low-lying $a^3\Sigma_g^+$, $b^3\Sigma_u^+$, and $c^3\Pi_u$, states which are shown in Fig. 3. Differential cross sections for these first two states have been calculated by Kuppermann and Cartwright[6] using the Ochkur-Rudge theory. In addition, Trajmar *et al.*[11] have measured the relative differential cross section for the $X^1\Sigma_g^+ \rightarrow b^3\Sigma_u^+$ transition which leads to dissociation. Also available are the Gryzinski estimates of Prok *et al.*[9] for a number of the triplet states in H_2. It is known, however, that the semiclassical Gryzinski calculations give overestimates of the triplet cross sections when compared to Ochkur-Rudge theory or experiment. This is because the Gryzinski cross sections are not determined by the wave functions of the states in question but rather by the relative position of the energy levels. We have therefore graphically integrated the differential cross-section data of Trajmar *et al.* for the $X^1\Sigma_g^+ \rightarrow b^3\Sigma_u^+$ transition and normalized the total cross section thus obtained to the Ochkur-Rudge calculations of Cartwright and Kup-

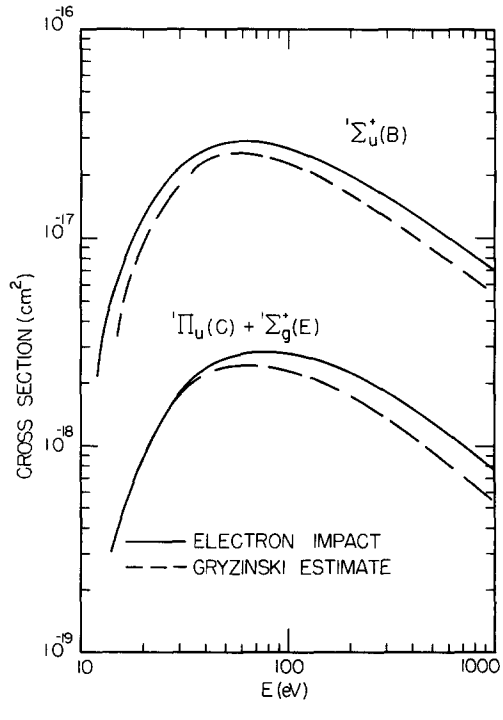

FIG. 2. Cross sections for the lowest singlet states in H_2. Solid lines refer to generated cross sections from electron-impact data. Dashed lines are taken from the semiclassical calculation of Prok *et al.* (Ref. 9).

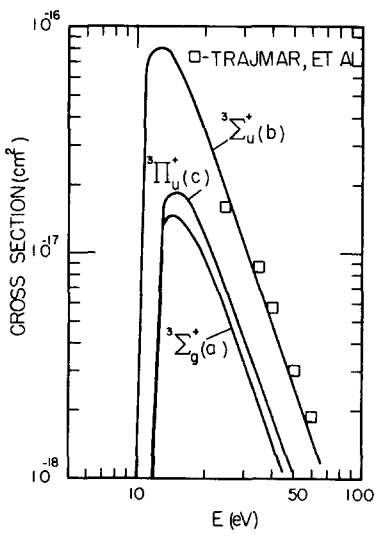

FIG. 3. Cross sections for the lowest triplet states in H_2. Solid curves represent fits of Eq. (10) to experimental and theoretical data (Refs. 6 and 11).

permann.[6] These have been found to give a good approximation to the total dissociation cross section[13] when corrected for ionization processes.[14] Once the differential data of Trajmar *et al.* is normalized it is possible to compare the relative magnitudes of the measured cross sections from the energy-loss spectrum to the corresponding Gryzinski estimates. This procedure indicates that the cross section calculated by Prok *et al.* is roughly five times that measured experimentally for the $c^1\Pi_u$ state. Although the Gryzinski estimates are seen to be somewhat unreliable, it is felt important to include the higher-energy triplet states, if only approximately, and a general reduction factor of one-fifth is used for all such states. The final values of the parameters used in representing the triplet cross sections are given in Table II. Prok *et al.*[9] also calculate a number of higher-energy singlet cross sections for H_2 which we incorporate into our work using the second form of Eq. (11) in conjunction with Eq. (10). No reduction factor is used for the singlets and the parameters are also contained in Table II.

Since a correct energy deposition study requires the knowledge of all the cross sections associated with an atom or molecule, it is useful to project cross sections of higher members of a Rydberg series from known information about the lower members. It is also of interest to see if one can relate singlet and triplet cross sections for states differing only by spin multiplicity (i.e., $S=0$ and $S=1$). Oscillator strengths f conform approximately to the rule[2]

$$f_n = f^*/(n-\delta)^3 , \tag{12}$$

where the quantum defect δ is determined by fitting the excitation energies to the usual formula

$$W_n = I - R_e/(n-\delta)^2 \tag{13}$$

and f^* is constant for a particular series. In addition, the spectrographic studies of Takezawa[15] on the absorption spectrum of H_2 provide information on the quantum defects for the transitions to the $np\sigma^1\Sigma_u^+$ and $np\pi^1\Pi_u$ states with $n=2, 3, 4, 5$. The quantum defects for these states are given as $\delta=-0.20$ and 0.08, respectively. The defect for the $^1\Sigma_g^+$ series is obtained by fitting to the excitation energies and δ is found to be -0.25. The quantum defects for the remaining Rydberg series should be small and are taken to be zero. It is now possible to lump together the higher members of a Rydberg series ($n > n'$) by replacing their sum by an integral and replacing the excitation energies by $W_R \approx \frac{1}{2}(W_{n'}+I)$. The sum of the remaining cross sections is then given by

$$\sigma_R = \frac{q_0 A^*}{2(n'-\delta)^2 W_R^2}\left(\frac{W_R}{E}\right)^{\Omega}\left(1-\frac{W_R}{E}\right)^{\nu} , \tag{14}$$

with $A^* = A(n-\delta)^3$.

An analysis of existing experimental and theoretical data was also undertaken for which a comparison of all singlet and triplet cross sections for a given set of quantum numbers could be made. The purpose of such an analysis is to enable us to give rough estimates when only one of the corresponding singlet-triplet cross sections is known. As a rough rule of thumb it was found that the singlet cross sections at 40 eV (three times threshold) were about two hundred times as large as the corresponding triplet cross section. Using Eqs. (10) and (11) with $E=3W$, it was then possible to relate the normalization constant A for the singlet and triplet cases. The final values of the parameters used to describe all the discrete states of H_2 are given in Table II.

III. IONIZATION CONTINUA

We next consider the important ionization processes in H_2. Again, Lassettre's data[5] on ionization thresholds is not well resolved so that only one ionization threshold ($I=15.42$ eV) is considered. We follow the work of Strickland and Green[16] whereby the differential oscillator strength df/dW is represented by a sum of analytic exponential functions. The parameters are chosen by means of a nonlinear least-squares fit to Lassettre's data. The distortion parameters used are the same as those obtained for helium.[17] The differential ionization cross section $S(E,W) \equiv d\sigma/dW$ is then simply obtained by integrating the differential oscillator strength, i.e.,

$$S(E,W) = \frac{q_0}{WE}\int \frac{1}{\xi}\frac{df}{dW}d\xi . \tag{15}$$

In the spirit of our representations for the discrete states of H_2, we now express $S(E,W)$ in the form

$$S(E,W) = \frac{q_0 A}{W^2}\left(\frac{I}{W}\right)^p\left(\frac{W}{E}\right)^{\Omega}\left(1-\frac{W}{E}\right)^{\nu} , \tag{16}$$

with $W = E_s + I$. Here I = ionization threshold, E = incident electron energy, and E_s = secondary electron energy. The actual ionization energy will vary depending upon the final vibrational state of the H_2^+ ion. We assume (judging from the Franck-Condon factors) that most of the H_2^+ ions are left in their ground state and choose an average $I=16.0$ eV. A, p, Ω, and ν are parameters to be fit to the data. It is found that reasonably good fits to the differential ionization cross sections are obtained with a value of $p=1.1$. It is this parameter which will have a critical effect on how the initial electron energy is dis-

TABLE II. Discrete states in H_2.

Singlets[a]					Triplets[b]				
(n)	Series	States	W (ev)	A	(n)	Series	States	W (eV)	A
	$^1\Sigma_g^+$ ($ns\sigma$)					$^3\Sigma_g^+$ ($ns\sigma$)			
2		E	12.40	0.0856	2		a	11.89	0.1250
3		H	14.12	0.0706	3		h	13.98	0.0005
4		0	14.86	0.0187	4		···	14.50	0.0003
$n>4$	$\delta=-0.25$		15.14	0.0396					
	$^1\Sigma_u^+$ ($np\sigma$)					$^3\Sigma_u^+$ ($np\sigma$)			
2		B	11.37	0.3267	2		b	10.00	0.5000
3		···	13.62	0.1000	3		e	13.36	0.0051
4		···	14.50	0.0238	4		f	14.47	0.0026
$n>4$	$\delta=-0.20$		14.96	0.0500					
	$^1\Pi_u$ ($np\pi$)					$^3\Pi_u$ ($np\pi$)			
2		C	12.40	0.2822	2		c	11.87	0.1600
3		D	14.12	0.0155	3		d	13.97	0.0065
4		···	14.57	0.0156	4		k	14.68	0.0005
$n>4$	$\delta=0.08$		15.00	0.0306					
	$^1\Sigma_g^+$ ($nd\sigma$)					$^3\Sigma_g^+$ ($nd\sigma$)			
3		G	13.98	0.0367	3		g	13.98	0.0007
4		P	14.82	0.0311	4		p	14.69	0.0003
$n>4$	$\delta=0.0$		15.12	0.0622					
	$^1\Pi_g$ ($nd\pi$)					$^3\Pi_g$ ($nd\pi$)			
3		I	14.02	0.0102	3		i	14.01	0.0005
4		R	14.72	0.0192	4		r	14.70	0.0013
$n>4$	$\delta=0.0$		15.07	0.0384					
	$^1\Delta_g$ ($nd\delta$)					$^3\Delta_g$ ($nd\delta$)			
3		J	14.06	0.0313	3		j	14.03	0.0039
4		S	14.86	0.0110	4		s	14.69	0.0002
$n>4$	$\delta=0.0$		15.14	0.0220					
	$^1\Pi_g$					$^3\Pi_g$ ($nf\pi$)			
		Q	14.20	0.1146	4		v	14.67	0.0047

[a]All singlet cross sections for H_2 are fit to Eqs. (10) and (11) with $\Omega=0.75$ and $\nu=3$. Rydberg states with $n>4$ and quantum defect δ are summed using Eq. (14).
[b]All triplet states for H_2 are fit to Eqs. (10) and (11) with $\Omega=3.0$ and $\gamma=3$.

tributed among the various possible secondary ion states.

Because of the convenient form chosen for $S(E, W)$, it is now possible to obtain the integrated ionization cross section

$$\sigma_{ION}=\int_I^{(E_s+I)/2} S(E, W)\,dW \quad . \tag{17}$$

In Fig. 4 we show the total ionization cross section taken from Rapp and Englander-Golden[14] together with the integrated differential cross sections generated from Lassettre's data. Here we find that inclusion of distortion effects tends to make our generated cross section fall somewhat below that of Rapp and Englander-Golden. In addition, the representation of all the ionization continua in H_2 as a single continuum is probably too much of an oversimplification. In order to partially resolve these discrepancies, we fit the integrated form of Eq. (16) directly to the total ionization data in Fig. 4. The final values of the ionization parameters are given in Table III.

IV. DISSOCIATION PROCESSES

A. Dissociative Excitations

Here we consider processes of the type

$$e+H_2 \rightarrow e+H_2^* \ ,$$

$$H_2^* \rightarrow H+H^* \ ,$$

i.e., where the molecule is dissociated into a ground- and excited-state atomic configuration. Recent measurements by Vroom and DeHeer[18] have made available absolute emission cross sections for atomic hydrogen in the $n=2$–6 excited states. The $n=2$ excited state has been studied by observing Lyman α radiation while the higher states ($n=3$–6) have been investigated by observation of Balmer radiation. In Fig. 5 we show cross sections for excitation of the $n=2$–6 excited states in hy-

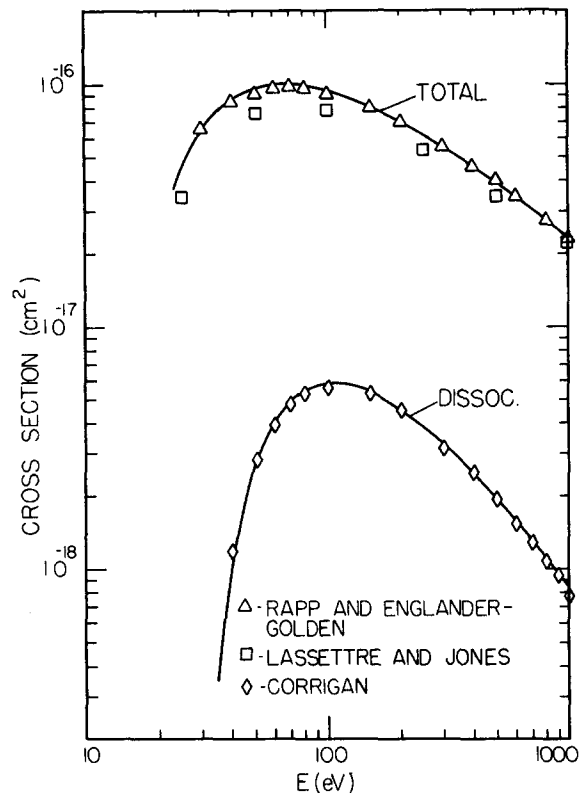

FIG. 4. Ionization cross sections for H_2. Solid curves represent fits to experimental data as discussed in text.

drogen by dissociation. The $n = 2$ cross section has been corrected for cascading by subtracting out the Balmer contributions. It is expected[18] that cascade effects in the Balmer series will be negligible.

We have included these dissociative excitation cross sections by fitting them to the discrete analytic form of Eq. (10). Although these are actually continum processes, lack of detailed information about the energy transfer prevents us from using a more precise representation. In order to take into account the higher excited states in the Balmer series leading to the ionization threshold, we have attempted to characterize them as members of a Rydberg series. It was found that the lower members of the Balmer series could be accommodated to a $1/(n-\delta)^3$ rule with $\delta \approx 2.0$. The final parameters describing the dissociative excitations in H_2 are given in Table IV.

B. Dissociative Ionization

Another important dissociation process to be considered is where one of the dissociation products is ionized. Here we are guided by the cross-section measurements of Englander-Golden and Rapp[19] for H_2 yielding product ions with kinetic energies greater than 2.5 eV as shown in Fig. 3. We can utilize data of this type by fitting to the integrated form of $S(E, W)$ given by Eq. (16). The resultant parameters are found in Table III.

V. VIBRATIONAL EXCITATION AND NEGATIVE ION FORMATION

While in atoms such as hydrogen, only electronic transitions are important, even in the simplest molecules such as H_2 the effects of nuclear motion through vibrational and rotational energy changes must also be taken into account. Schulz[20] has obtained cross sections for the $v = 1$ and $v = 2$ ground vibrational states shown in Fig. 6 and finds that the $v = 1$ state predominates (the peak cross section for the $v = 2$ state is approximately 14% of the peak cross section for the $v = 1$ state). Although the $v = 1$ cross section is relatively large, its very low threshold and sharp drop off will cause it to play an important role only in the very low-energy behavior of the electron loss function.

In attempting to explain the rather large vibrational cross section, Chen and Magee[21] have investigated the role of the compound $H_2^-(^2\Sigma_u^+)$ state in vibrational excitation by electron impact. They show that the formation of a transient H_2^- ion as an intermediate state gives rise to a large cross section ($\sim 10^{-16}$ cm^2) for vibrational excitation of H_2 in the 6–8-eV energy range. A search by Schulz[20] in that region proved fruitless but of interest is the fact that the observed $v = 1$ cross section is in reasonable agreement with theoretical predictions. We have included the first two vibrational levels through use of the discrete representation given by Eq. (10). The final parameters for the vibrational states are found in Table V.

TABLE III. Analytic cross-section parameters for ionization continua.

Process	I (eV)	Ω	A	p	ν
Direct ionization	15.42	0.81	0.22	1.1	1
Dissociative ionization	28.00	1.55	0.01	1.1	2

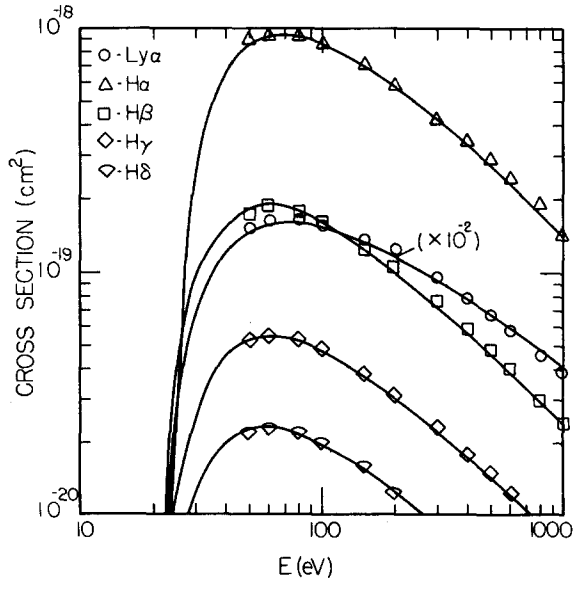

FIG. 5. Dissociative excitation cross sections for H_2. Solid curves represent fits to experimental data as discussed in text.

TABLE IV. Analytic cross-section parameters for dissociative excitation processes.

State	$\overline{W}_d$ (eV)[a]	W_{fit} (eV)[b]	Ω	A	ν
H(1s)+H ($n=2$)	17.0	20.0	0.75	0.500	2
H(1s)+H ($n=3$)	19.0	23.0	1.00	0.052	2
H(1s)+H ($n=4$)	20.0	20.0	1.00	0.008	2
H(1s)+H ($n=5$)	20.5	20.5	1.00	0.002	2
H(1s)+H ($n=6$)	21.0	19.5	1.00	0.001	2
H(1s)+H ($n>6$)	21.0	···	1.00	0.002	2

[a]Refers to the estimated energy loss for the process.
[b]W_{fit} has been chosen to achieve a good fit with Eq. (10) and is not directly related to $\overline{W}_d$.

VI. LOSS FUNCTION FOR H_2

Once cross sections are known for all important inelastic processes it is then possible to construct the loss function (stopping power) for H_2. The loss function is defined as

$$L(E) = -n^{-1}\frac{dE}{dx} \tag{18}$$

and represents an energy loss per unit path length. For an electron of energy E incident on a single species with concentration n, $L(E)$ can be written as a sum

$$L(E) = \sum_j \sigma_j(E) W_j + \sum_i \int_I^{(E+I)/2} W S_i(E, W)\, dW + \sum_d \overline{W}_d \sigma_d(E) \quad . \tag{19}$$

Here the successive terms represent the loss contribution due to excitation of atomic or molecular states with excitation energies W_j, ionizations with threshold energies I, and finally dissociations in the dth continuum with dissociation energy $\overline{W}_d = E_d + \overline{T}_d$, where E_d is the threshold and $\overline{T}_d$ the average kinetic energy of the products.

With our set of analytic cross sections we can now calculate the total loss function $L(E)$ for H_2 using the parameters given in Tables II–V. In Fig. 7 we show the calculated H_2 loss function together with a value calculated by Berger and Seltzer[22] at 10 000 eV based upon the expression for stopping power due to Bethe which involves a phenomenologically adjusted parameter.

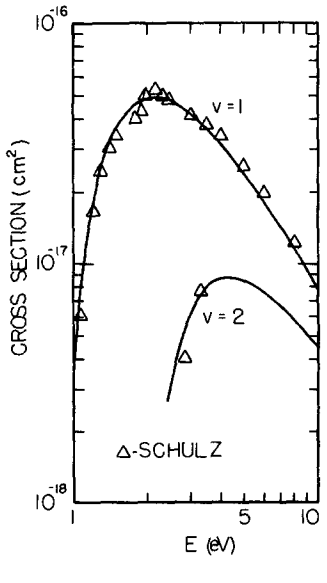

FIG. 6. Cross sections for the $v=1$ and $v=2$ ground vibrational states in H_2. Solid curves represent fits to experimental data as discussed in text.

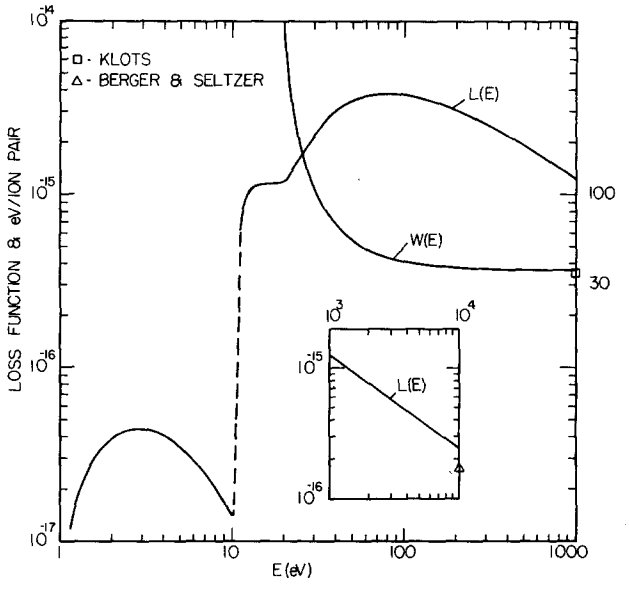

FIG. 7. $L(E)$ denotes loss function for H_2 (left scale). $W(E)$ denotes the eV/ion pair (right scale). Dashed line indicates lack of reliable cross-section data below 10 eV.

VII. EFFICIENCIES

Once $L(E)$ is known, it then becomes possible to trace the complete degradation of an electron with some incident energy E. Such a calculation is carried out within the continuous-slowing-down approximation[3] (CSDA) which assumes that it is possible to replace discrete energy losses by a continuous function. Such an approximation has been found to be satisfactory[23] except, possibly, at very low energies where only a few collisions may use up the energy of the primary. In order to adapt the loss function for use in calculating ionization yields, we express $L(E)$ in a form used by Green and Peterson[24] to characterize a number of atmospheric gases:

$$L(E) = \frac{q_0 Z}{2R_e}\left[\left(\frac{E}{A}\right)^{\Omega} + \left(\frac{E}{B}\right)^{M} + \left(\frac{E}{C}\right)^{\Lambda}\right]^{-1} \quad . \tag{20}$$

Here Z, B, C, Ω, M, and Λ are adjustable parameters to be fit to the data and are given in Table VI.

TABLE V. Analytic cross-section parameters for vibrational states.

State	W (eV)[a]	W_{fit} (eV)[b]	Ω	A	ν
$X^1\Sigma_g^+$ ($v=1$)	0.53	0.80	2.0	0.018	3
$X^1\Sigma_g^+$ ($v=2$)	1.06	1.80	2.0	0.010	3

[a]Refers to the estimated energy loss for the process.
[b]W_{fit} has been chosen to achieve a good fit with Eq. (10) and is not directly related to W.

TABLE VI. Analytic parameters for the loss function.

Z	Ω	M	Λ	A	B	C
5.03	0.823	0.125	−1.950	100.0	60.0	0.8

The final parameters of interest in the particle degradation problem are the efficiencies of energy deposition in various processes. For excitations these take the form

$$P_j(E_p) = P_{oj}(E_p) + \int_0^{(E_p-I)/2} P_j(T) n_T(E_p, T)\, dT \quad , \tag{21}$$

with

$$P_{oj} = (W_j/E_p) \int_{W_j}^{E_p} \sigma_j(E)/L(E)\, dE \quad . \tag{22}$$

In Eq. (21), n_T represents the secondary electron spectrum given by

$$n_T(E_p, T) = \sum_i \int_{2T+I_i}^{E_p} S_i(E, W)/L(E)\, dE \quad , \tag{23}$$

with T the energy of the secondary electron. The first term in Eq. (21) gives the efficiency due only to the primary electron. The second term represents the contributions from secondaries and higher-order electrons. Dissociative and ionization efficiencies can be represented in a similar way. Further details can be found in Ref. 3. From the ionization yield one can also calculate the quantity

$$W(E) = I/P_{\mathrm{ION}}(E) \quad , \tag{24}$$

the "eV per ion pair". $W(E)$ is known to approach a constant value at high energies and is shown in Fig. 7 together with the experimentally reported value listed by Klots.[25] Efficiencies for the various processes considered are shown in Fig. 8.

VIII. SUMMARY AND CONCLUSION

We have presented a detailed set of electron-impact cross sections characterizing the fundamental processes initiated by electrons in molecular hydrogen. Our input cross sections were based primarily on experimental information and phenomenological extensions of the Born approximation into the low-energy region. Although many of our cross-section rules are an outgrowth of earlier phenomenological studies of helium, recent studies[26–29] using a realistic independent-particle model lend support to this approach. The final efficiencies for the various processes shown in Fig. 8 are, of course, no better than the input cross sections. Therefore, our results should be examined in the light of experimental observations on energy deposition with the hope of eventually achieving reasonable self-consistency.

Our set of analytic cross sections should also be useful as input for detailed calculations on stimulated-emission transition probabilities and laser power densities in molecular hydrogen. Laser action in the Lyman band ($B^1\Sigma_u^+ \rightarrow X^1\Sigma_g^+$) has been observed[4] near 1600 Å and is obtained by inverting the population of an excited electronic state with respect to the high vibrational-rotational levels of the ground state. Stimulated emission in H_2 was proposed initially by Bazhulin, Knyazev, and Petrash[30] on the Werner band transitions ($C^1\Pi_u \rightarrow X^1\Sigma_g^+$) in the 1100-Å region and this proposal was then followed by a detailed rate-equation analysis by Ali and Kolb[31] who predicted spectral lines between 1025–1239 Å. Such a calculation has not been carried out for the Lyman band.

In order to solve the rate equations governing the laser power density and the population densities of the various vibrational levels, it is necessary to know electron-impact excitation rate coefficients for the various transitions. These can be simply obtained using our convenient analytic cross sections averaged over a Maxwellian velocity distribution. In addition, when calculating the laser power density, it is important to take into account all pertinent energy-loss processes and, in particular, the excitations to the important low-lying triplet states which will greatly reduce laser power density. The efficiencies in Fig. 8 show that these processes are predominant at low energies (~ 11 eV).

Another interesting application of the present work is to make approximate estimates of impact cross sections for heavier particles, in particular, protons. The study of Green and McNeal[32] indicates that most of the important cross sections for collisions of protons and hydrogen atoms with atomic and molecular gases can be systematized using analytic expressions which reduce to the well-known Born approximation. Once the basic proton cross sections are known, it should be possible to apportion the incident proton energy into the various secondary-electron, ionization, and direct-excitation processes. At this point one could then take advantage of the present degradation results for molecular hydrogen

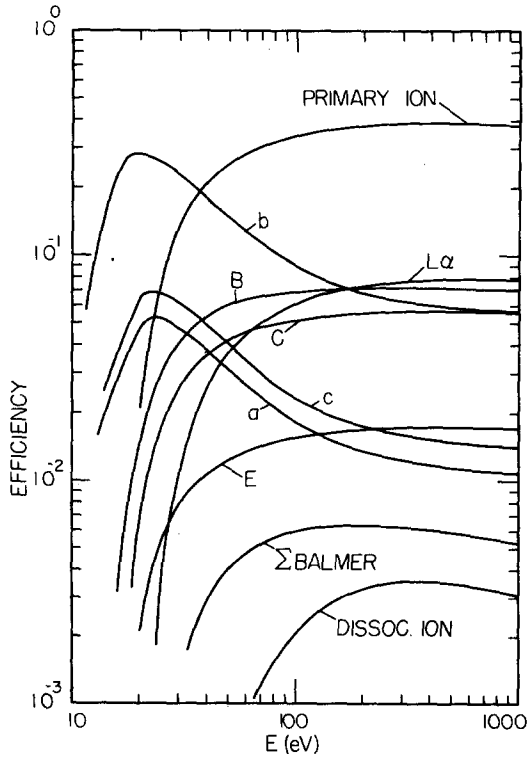

FIG. 8. Efficiencies for electron energy deposition in H_2.

since the further degradation of the low-energy secondary electrons would proceed analogously to electron-stimulated events.

Finally we call attention to the importance of a knowledge of H_2-impact cross sections to planetary aeronomy, in particular, to studies of the Jovian atmosphere in which H_2 is the predominant species. In this connection, after the present work was completed, a study of molecular hydrogen motivated by this application by Takayanagi and Nakata[33] (TN) became available. The major portion of the TN study is devoted to a comprehensive review of the various processes initiated by electron impact with particular attention to elastic scattering and rotational and vibrational excitations. The second half of the TN work makes use of the known H_2 cross-section data including a number of electronic excitations to calculate photoelectron production as well as Lyman α and Balmer α emission rates in the Jovian upper atmosphere using CSDA. In order to carry out such calculations, the authors proceed in a manner similar to that of the present work, i.e., identifying the predominant energy-loss mechanisms in H_2 and then utilizing available cross-section data or estimates to construct the associated loss function (stopping cross section). Their differential ionization cross section is based upon a semiempirical formula for secondary electrons due to Khare.[34] On the whole, the TN loss function is quite similar to our loss function agreeing precisely at 200 eV. At low energies they are somewhat higher (e.g., a factor of 2 at 30 eV) but at higher energies they are somewhat lower (e.g., a factor of 0.6 at 1 keV). The former discrepancy is probably due to the use of simple Born cross sections for the singlet B and C states whose values between 10–30 eV are three times as large as our distorted cross sections. The latter discrepancy arises primarily because they do not include the higher allowed electronic states (including Rydberg series) and the higher dissociative excitation states which for the sake of completeness have been included here. If one considers the general state of knowledge of electronic excitation, dissociation, and ionization cross sections in the region of importance to most applications (i.e., below the range of validity of the Born-Bethe approximation), the over-all agreement between the two loss functions is probably of greater significance than the disagreements. Since TN do not calculate efficiencies which should be of particular interest in application to H_2 lasers, further detailed comparisons are not possible.

ACKNOWLEDGMENTS

The authors would like to thank Dr. L. R. Peterson, Dr. J. J. Olivero, Dr. T. Sawada, and Dr. R. Stagat for helpful discussions.

*Supported in part by the United States Atomic Energy Commission.

†Present address: Drexel University, Philadelphia, Pa. 19100.

[1]H. Bethe, Ann. Phys. (Paris) 5, 325 (1930).
[2]A. E. S. Green, and S. K. Dutta, J. Geophys. Res. 72, 3933 (1967).
[3]L. R. Peterson and A. E. S. Green, J. Phys. B 1, 1131 (1968).
[4]R. T. Hodgson, Phys. Rev. Letters 25, 494 (1970).
[5]E. N. Lassettre and E. A. Jones, J. Chem. Phys. 40, 5 (1964).
[6]D. C. Cartwright and A. Kuppermann, Phys. Rev. 163, 163 (1967).
[7]R. H. Thompson and K. J. Casper, Nucl. Phys. 72, 106 (1965).
[8]K. J. Miller and M. Krauss, J. Chem. Phys. 47, 10 (1967).
[9]G. M. Prok, C. F. Monnin, and H. J. Hettel, NASA Report No. Tn D-4004, 1967 (unpublished).
[10]M. Gryzinski, Phys. Rev. 138, 336 (1965).
[11]S. Trajmar, D. C. Cartwright, J. K. Rice, R. T. Brinkmann, and A. Kuppermann, J. Chem. Phys. 49, 5464 (1968).
[12]A. E. S. Green and C. A. Barth, J. Geophys. Res. 70, 1083 (1965).
[13]S. J. B. Corrigan, J. Chem. Phys. 43, 4381 (1965).
[14]D. Rapp and P. Englander-Golden, J. Chem. Phys. 43, 1464 (1965).
[15]S. Takezawa, J. Chem. Phys. 52, 2575 (1970).
[16]D. J. Strickland and A. E. S. Green, J. Geophys. Res. 74, 6415 (1969).
[17]A. T. Jusick, C. E. Watson, L. R. Peterson, and A. E. S. Green, J. Geophys. Res. 72, 3943 (1967).
[18]D. A. Vroom and F. J. DeHeer, J. Chem. Phys. 50, 580 (1969).
[19]P. Englander-Golden and D. Rapp, Lockheed Missiles and Space Co. Report No. LMSC-6-74-64-12, 1964 (unpublished).
[20]G. J. Schulz, Phys. Rev. 135, A988 (1964).
[21]J. C. Y. Chen and J. L. Magee, J. Chem. Phys. 36, 1407 (1962).
[22]M. J. Berger and S. M. Seltzer, National Academy of Sciences-National Research Council Publication No. 1133, 1964 (unpublished).
[23]L. R. Peterson, Phys. Rev. 187, 105 (1969).
[24]A. E. S. Green and L. R. Peterson, J. Geophys. Res. 73, 233 (1968).
[25]C. E. Klots, *Fundamental Processes in Radiation Chemistry*, edited by Peter Ausloos (Interscience, New York, 1968), Chap. 1.
[26]A. E. S. Green, D. L. Sellin, and A. S. Zachor, Phys. Rev. 184, 1 (1969).
[27]P. S. Ganas, S. K. Dutta, and A. E. S. Green, Phys. Rev. A 2, 111 (1970).
[28]P. S. Ganas and A. E. S. Green, Phys. Rev. A 4, 182 (1971).
[29]T. Sawada, J. E. Purcell, and A. E. S. Green, Phys. Rev. A 4, 193 (1971).
[30]P. A. Bazhulin, I. N. Knyazev, and G. G. Petrash, Sov. Phys. JETP 21, 649 (1965).
[31]A. W. Ali and A. C. Kolb, Appl. Phys. Letters 13, 259 (1968).
[32]A. E. S. Green and R. J. McNeal, J. Geophys. Res. 76, 133 (1971).
[33]K. Takayanagi and K. Nakata, Bull. Inst. Space Aeronaut. Sci. 6, No. 4, 849 (1970).
[34]S. P. Khare, Planetary Space Sci. 17, 1257 (1969).